Journal of Magnetic Resonance 212 (2011) 95–101

Contents lists available at ScienceDirect

Journal of Magnetic Resonance

journal homepage: www.elsevier.com/locate/jmr

Cross-correlations between low-γ nuclei in solids via a common dipolar bath

Aanatoly K. Khitrin [a,b], Jiadi Xu [a], Ayyalusamy Ramamoorthy [a,*]

[a] Biophysics and Department of Chemistry, The University of Michigan, Ann Arbor, MI 48109-1055, USA
[b] Department of Chemistry and Biochemistry, Kent State University, Kent, OH 44240-0001, USA

ARTICLE INFO

Article history:
Received 11 March 2011
Revised 11 June 2011
Available online 20 July 2011

Keywords:
Cross-correlations
Dipolar bath
Static NMR
Bio-solids
Resonance assignment

ABSTRACT

Correlation of chemical shifts of low-γ nuclei (such as ^{15}N) is an important method for assignment of resonances in uniformly-labeled biological solids. Under static experimental conditions, an efficient mixing of low-γ nuclear spin magnetization can be achieved by a thermal contact to the common reservoir of dipole–dipole interactions in order to create ^{15}N–^{15}N, ^{13}C–^{13}C, or ^{15}N–^{13}C cross-peaks in a 2D correlation spectrum. A thermodynamic approach can be used to understand the mechanism of magnetization mixing in various 2D correlation pulse sequences. This mechanism is suppressed under magic-angle spinning, when mixing via direct cross-polarization with protons becomes more efficient. Experimental results are presented for single-crystalline and powder samples of ^{15}N-labeled *N*-acetyl-L-^{15}N-valyl-L-^{15}N-leucine (NAVL). In addition to the thermodynamic analysis of mixing pulse sequences, two different new mixing sequences utilizing adiabatic pulses are also experimentally demonstrated.

1. Introduction

Correlation spectroscopy in solids can provide valuable information about the proximity of low-γ nuclei such as ^{13}C and ^{15}N. Cross-correlations can be created by a direct dipolar coupling between a pair of homonuclear spins. This coupling allows a flip-flop motion of the spins, leading to a transfer of magnetization and spin diffusion. Since magic-angle spinning (MAS) averages out the homonuclear dipolar coupling, dipolar recoupling sequences are used to enable the polarization transfer among low-γ nuclear spins under MAS. Numerous recoupling schemes have been developed to enable the polarization transfer under MAS [1–6]. Protons can facilitate the polarization transfer, as it is known from traditional proton-driven spin diffusion (PDSD) [7–9] or more advanced PARIS [6] experiments. All recoupling techniques, proton-assisted or not, rely on a direct coupling between low-γ nuclei. When the direct coupling is weak, a build-up of cross-correlations is slow. For example, direct ^{15}N–^{15}N dipolar coupling among amide-^{15}N nuclei in polypeptides is so small that a mixing time on the order of seconds is required [10,11]. Therefore, a large effort has been devoted to speed up the spin diffusion process among low-γ nuclei. The most common approach is transferring the magnetization to protons and then back to low-γ spins under stationary [12] or magic angle spinning conditions [13–16].

Recently, several efficient solid-state NMR techniques [17–21], implementing this two-step polarization transfer, have been proposed for creating cross-correlations between ^{15}N or ^{13}C nuclei with very weak direct dipolar coupling. In fact, these techniques do not require a direct coupling between low-γ nuclei and, with a small modification, can be used for producing heteronuclear cross correlations, e.g. between ^{15}N and ^{13}C nuclei. Despite different names: cross-relaxation driven spin diffusion (CRDSD) [17], mismatched Hartmann–Hahn (MMHH) [18,19], or proton-assisted recoupling (PAR) [20,21], the techniques share a common basic mechanism. A common mechanism for the mixing of low-γ nuclear spin magnetization for both the published pulse sequences [17–21] and the new ones is described in this study. It is shown that, for static samples, the most efficient mechanism of mixing is the thermodynamic coupling to a common reservoir of dipole–dipole interactions. Under MAS condition, the major mechanism is a conventional cross-polarization (CP). Experimental results obtained from single-crystalline and powder samples of ^{15}N-labeled *N*-acetyl-L-^{15}N-valyl-L-^{15}N-leucine (NAVL) are presented.

2. Theory

A theoretical analysis of several mixing schemes is presented in this section. We consider static samples, except for a brief discussion of MAS at the very end of this section. Let us start with the CRDSD pulse sequence given in Fig. 1a. The *S*-spin magnetization (^{15}N or ^{13}C), created by cross-polarization from *I* spins (protons), evolves under the chemical shift during t_1, and then it is locked for mixing by a spin-lock radio-frequency pulse. In the rotating frame, the Hamiltonian for this mixing period is

$$H = H_d - \omega_1 \Sigma_i S_{iX}, \quad H_d = H_{II} + H_{IS}, \tag{1}$$

where H_{II} is the Hamiltonian for the dipole–dipole interaction between *I* spins, H_{IS} is the heteronuclear dipole–dipole interaction Hamiltonian, and ω_1 is the strength of the applied spin-lock

* Corresponding author.
E-mail address: ramamoor@umich.edu (A. Ramamoorthy).

1090-7807/$ - see front matter © 2011 Elsevier Inc. All rights reserved.
doi:10.1016/j.jmr.2011.06.015

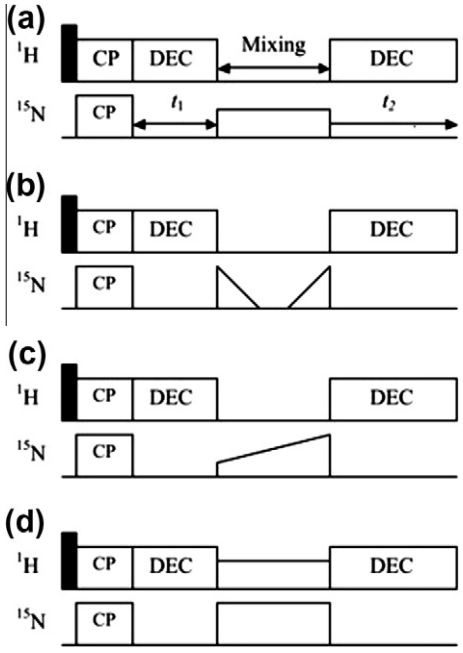

Fig. 1. Radio-frequency pulse sequences to correlate the chemical shifts of rare nuclear spins: (a) cross-relaxation driven spin diffusion (CRDSD) [9]; (b) with ramped adiabatic demagnetizing and remagnetizing pulses; (c) CRDSD with a ramped spin-lock mixing pulse; (d) a mismatched Hartmann–Hahn (MMHH) mixing [18,19] or a proton-assisted recoupling (PAR) [20,21].

radio-frequency field. The direct dipolar coupling between low-γ S spins is neglected as the ^{15}N–15N dipolar coupling between amide-^{15}N nuclei in a protein is very small. The heteronuclear dipole–dipole interaction H_{IS} contains only the z-components of I and S spins and, therefore, does not provide a direct mechanism for their flip-flop. Due to flip-flop motions of I spins driven by the Hamiltonian H_{II}, z-fields on S spins fluctuate causing transitions of the locked S spins, and thereby changing the magnetization of S spins along the x-axis of the rotating frame. The Hamiltonian (1) does not depend on time, and the total energy $\langle H \rangle$ is conserved. Therefore, any change in the Zeeman energy of S spins (in the rotating frame) $\omega_1 \Sigma_i \langle S_{iX} \rangle$ is compensated by corresponding change in the dipolar energy $\langle H_d \rangle$. These changes occur until the system reaches an equilibrium state described by a common spin temperature. The process of equilibration is very similar to the one in homonuclear spin-locking experiment described in detail by Goldman [22]. The only difference is expected for small concentrations of spins S where the equilibration becomes a two-step process. First, an equilibrium is established with nearby I spins, then the dipolar order propagates to larger distances by spin-diffusion [23].

In order to estimate the efficiency of building cross-correlations, we assume that only one S_1 spin is polarized at the beginning of the mixing period and calculate equal x-polarizations of S spins at the end of the equilibration process. The density matrix changes from the initial ρ_{in} to equilibrium ρ_{eq} as given below.

$$\rho_{in} = (Tr1)^{-1}(1 + \alpha\omega_1 S_{1X}) \rightarrow \rho_{eq} = (Tr1)^{-1}(1 + \beta(\omega_1 \Sigma_i S_{iX} - H_d)), \quad (2)$$

where α and β are the initial and final (inverse) spin temperatures. By introducing the local dipolar fields ω_L [22] on spins I and neglecting the heteronuclear contribution to the dipolar energy (a lower concentration of S spins, when compared to I spins, is assumed), one can calculate the initial E_{in} and final E_{eq} energies as

$$E_{in} = \alpha\omega_1^2/4 = E_{eq} = \beta(N_S\omega_1^2 + N_I\omega_L^2)/4, \quad (3)$$

where N_S and N_I are the number of S and I spins, respectively, in the sample per one S_1 spin. The efficiency p of cross-correlation can be calculated from Eq. (3) as

$$p = \beta/\alpha = \left(N_S + N_I\omega_L^2/\omega_1^2\right)^{-1} \quad (4)$$

This quantity is the final x-polarization of each of the S spins created from one unit of initial x-polarization of the S_1 spin. One can see that the efficiency decreases under the dilution of S spins: either in the presence of a larger number of protons or non-equivalent S spins. One can also realize that, for a higher efficiency, it is desirable to use a larger RF field strength (ω_1) for the spin-lock (in Fig. 1a). However, there is a kinetic limitation on the use of ω_1 values. The rate of approaching the equilibrium can be calculated as [22]

$$W \approx \omega_{LS}^2 g(\omega_1), \quad (5)$$

where ω_{LS} is the amplitude of the local dipolar z-field created by I spins on S spins and $g(\omega)$ is a normalized spectrum of time fluctuations of these z-fields at frequency ω. $g(\omega)$ describes a frequency spectrum of flip-flops in the I spin system. The width of this function is comparable, but somewhat narrower, than that of the dipolar-broadened spectrum of I spins. Therefore, when ω_1 is large compared to the width of $g(\omega)$, the rate W of the Zeeman-dipolar equilibration is slow.

The mixing period of the CRDSD pulse sequence given in Fig. 1a consists of three processes: (a) transfer of the Zeeman order of S spins to the dipolar order, (b) propagation of the dipolar order by spin diffusion of I spins, and (c) transfer of the dipolar order back to the Zeeman order of S spins. These three processes can also be achieved by the adiabatic demagnetization–remagnetization scheme shown in Fig. 1b. The first spin-lock pulse (in Fig. 1b) with decreasing amplitude locks the x-magnetization of S spins and gradually converts it to the dipolar order of the entire system. The dipolar order then propagates via the flip-flops of I spins. Finally, the remagnetization pulse with increasing amplitude converts the dipolar order into x-magnetization of S spins. The mechanism of converting the dipolar order to magnetization of rare spins has been studied in detail in the context of adiabatic cross-polarization (CP) [24].

The mixing mechanism discussed above also suggests how one can improve the efficiency of the scheme given in Fig. 1a. At the beginning of the mixing period, it is desirable to convert more polarization into the dipolar order for subsequent fast propagation through the system. At the end of the mixing period, it is beneficial to create a higher Zeeman order for S spins. Therefore, one expects that replacing the spin-lock pulse of constant amplitude by a ramped pulse with increasing amplitude, as shown in Fig. 1c, will enhance the cross-correlation efficiency.

The scheme shown in Fig. 1d uses a mismatched Hartmann-Hahn (MMHH) CP in the mixing period [18,19]. The scheme was also named as the proton-assisted recoupling (PAR), when applied under the magic angle spinning (MAS) condition [20,21]. Two spin-lock fields here have different amplitudes ω_{1S} and ω_{1I}. (The scheme in Fig. 1a can be viewed as a variant of this sequence at $\omega_{1I} = 0$.) The mechanism of creating the dipolar order by the sequence given in Fig. 1d is similar to the one discussed above for the pulse sequence given in Fig. 1a. The differences are the following. Cross-polarization in the doubly-rotating frame (quantization axis is x) is governed by zero-quantum interactions, $S^+I^- + S^-I^+$, providing flip-flops between I and S spins in the rotating frame. At the exact match condition, $\omega_{1S} = \omega_{1I}$, flip-flops conserve the energy. When $\omega_{1S} \neq \omega_{1I}$, the energy difference $(\omega_{1S} - \omega_{1I})$ goes to the reservoir of dipole–dipole interactions and changes its spin temperature. The dipolar bath itself is also modified by a strong field ω_{1I}: the dipolar interaction H_{II} is truncated to $-(1/2)H_{XII}$, where H_{XII} has the same form as H_{II} except that the x- and z-axes are inter-

changed. Depending on the parameters, the scheme in given Fig. 1d can also convert the Zeeman order of S spins to the Zeeman order of I spins and back. This type of mixing would be especially efficient when two S spins are directly coupled to a common I spin. In this case, the mechanism can be viewed as the third-spin assisted recoupling (TSAR) [25].

So far, we have considered a static sample. The pulse sequence given in Fig. 1d has already been successfully tested under fast magic-angle spinning (MAS) [20,21]. MAS averages out dipolar interactions and, therefore, the dipolar reservoir disappears. Besides mixing via the Zeeman reservoir of I spins, there is potentially one more possibility. As it has been demonstrated elsewhere [26], a long-lived pseudo-dipolar order can exist under fast MAS. It has been shown [26] that non-averaged multi-spin effective interactions form a reservoir of pseudo-dipolar couplings, which can be treated very similar to the dipolar reservoir for static solids. In particular, transfer of the Zeeman order to and from the pseudo-dipolar order can be observed in the same set of experiments: off-resonance saturation or two-pulse Jeener–Broekaert sequence [27]. The experimental observation of the transfer of pseudo-dipolar order to the Zeeman order is reported [28,29]. The strength of the pseudo-dipolar couplings can be guessed from the width of the central band of the proton spectrum under MAS. Under fast MAS, it can only be a few percent of the original static line width. Accordingly, the offsets, leading to the creation of the dipolar order in the experiments shown in Fig. 1, should be scaled down. For example, it could be expected that the maximum performance of the MMHH mixing is reached for offset $(\omega_{1S} - \omega_{1I})$ values close to the width of the central band of the proton MAS spectrum for the central-band CP, or similar offsets from the first spinning sideband matching. Unfortunately, we were unable to directly observe mixing via pseudo-dipolar couplings in our experiments described in the next section.

The mechanism of creating cross-correlations discussed above is certainly not limited to homonuclear spins. For example, to create a correlation among ^{15}N and ^{13}C nuclei, one can first convert the Zeeman order of ^{15}N to the dipolar order and then the dipolar order to the Zeeman order of ^{13}C. The modification of the pulse sequences shown in Fig. 1 to accomplish correlation of heteronuclei is straightforward.

An important fact, that makes the above-discussed mechanism possible, is the presence of a common dipolar reservoir in heteronuclear spin systems [22]. Even if one type of low-γ spins is dilute, so that these spins do not interact between themselves and do not change their z-components, the flip-flops of abundant spins (protons) are sufficient to establish a common dipolar spin temperature. Thus the insights into the mechanism of magnetization mixing provided here suggest that numerous modification of CRDSD (given in Fig. 1a) is possible; pulse sequences given in Fig. 1b–d are essentially modifications of Fig. 1a. They can be grouped together by the mechanism of mixing – the ZDZ-mixing (Zeeman–Dipolar–Zeeman).

3. Experimental results and discussion

3.1. Static sample

A single crystal of uniformly ^{15}N labeled dipeptide *N*-acetyl-L-^{15}N-valyl-L-^{15}N-leucine (NAVL) at an arbitrary orientation with respect to the external magnetic field was used to demonstrate the pulse sequences shown in Fig. 1. All NMR experiments were performed at 15 °C. The sample preparation and molecular structure of NAVL are described in the literature [17]. There are two NAVL molecules per unit cell; so, the 1D ^{15}N chemical shift spectrum obtained under proton decoupling (SPINAL-64 [31]) consists of four peaks (shown in Fig. 2). The large distance between ^{15}N atoms in a crystal makes the direct coupling to be negligibly small (<30 Hz), so that the direct nitrogen flip-flops are totally suppressed by the chemical shift difference. For the chosen NAVL crystal orientation in Fig. 2, no cross peaks were observed in the PDSD-based 2D ^{15}N–15N correlation spectra obtained using a mixing time as large as 4 s.

Fig. 3 shows 2D ^{15}N–15N chemical shift correlation spectra obtained using the pulse sequences given in Fig. 1a–d with a 10 ms mixing time. The observation of cross peaks in these spectra clearly demonstrates similar high efficiency of all four pulse sequences in establishing ^{15}N–15N cross-correlations. All cross peaks, both intra- and inter-molecular, are fully developed after only 10 ms mixing. In fact, the intensities of the cross peaks are already saturated, which can be clearly seen in the traces shown in Fig. 4. The intensities of cross-peaks and diagonal peaks are comparable. It should be mentioned that the performance of the pulse sequences shown in Fig. 1a and d has also been studied for a single crystal of NAVL in a recent work [32].

Equally high performance of all the pulse sequences shown in Fig. 1 is based on the common mechanism. Namely, the transfer of the ^{15}N Zeeman order to the common dipolar reservoir of protons and nitrogens and then back to the nitrogen polarization. Below, we present more experimental evidence supporting this mechanism. It is mentioned in the recent reports [18,32] that the CRDSD pulse sequence given in Fig. 1a relies on the direct coupling between nitrogen nuclei, while the pulse sequence in Fig. 1d does not require the direct coupling. This is disproved by our results (Figs. 3 and 4) which suggest that the pulse sequence given in Fig. 1a does not require the low-γ nuclei to be dipolar-coupled, just like it is not required for the other pulse sequences in Fig. 1.

It has been shown that the dipolar order can also be created by adiabatically demagnetizing protons [30]. For protons, we used a 90°-pulse followed by a demagnetizing spin-lock pulse with a linear decrease in the amplitude. Adiabatic demagnetization of protons is fast and therefore the demagnetizing pulse can be as short as 0.5 ms. A subsequent spin-lock pulse on ^{15}N establishes a Zeeman-dipolar contact leading to an equilibrium (described by Eq. (2)) and, therefore, creating the ^{15}N magnetization. The situation for the second step is very similar to the one described by Eqs. (2)–(4) except that the initial order is now the dipolar order. Again, we expect that the ^{15}N magnetization will reach maximum when the spin-lock amplitude ω_{1S} is close to the dipolar coupling frequencies. Experimental results are presented in Fig. 5. For a 6 ms mixing time, peaks 1, 3, and 4 reach a maximum at ω_{1S}/

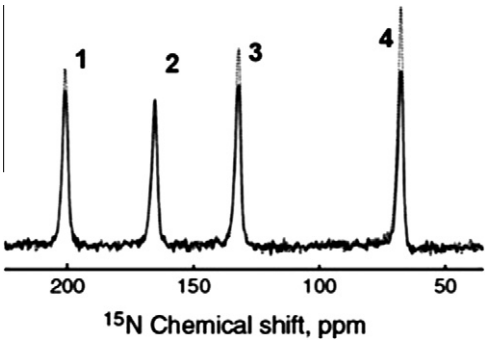

Fig. 2. 1D ^{15}N chemical shift spectrum of an NAVL single crystal with an arbitrary orientation relative to the external magnetic filed recorded using a ramped CP sequence (80% ramp, solid line) and adiabatic CP [24,30] (dots line). A 55 kHz SPINAL-64 decoupling was applied during acquisition for both sequences. 1 ms CP time and 37 kHz spin-lock field were used in ramp-CP; whereas a 1 ms ramp down pulse (from 40 kHz to zero) was applied for proton demagnetization and 6 ms ramp up pulse (from zero to 37 kHz) was used for ^{15}N remagnetization in adiabatic CP.

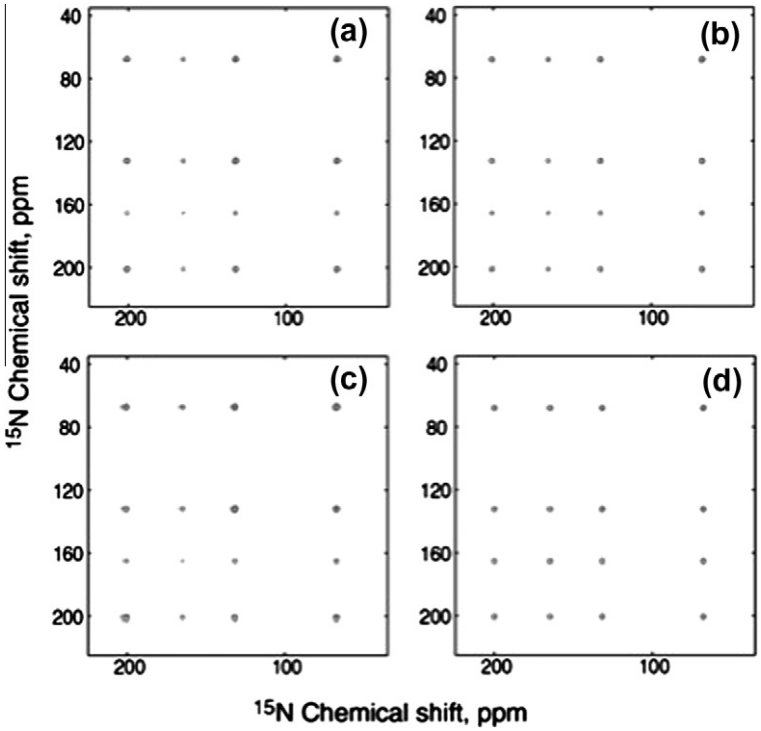

Fig. 3. (a–d) 2D ^{15}N–^{15}N correlation spectra of an NAVL single crystal recorded using the pulse sequences shown in Figs. 1a–d, respectively, with a 10 ms total mixing time; (a) the ^{15}N spin-lock field $\omega_{1S}/2\pi$ = 13.3 kHz; (b) two 3 ms ramped spin-lock pulses with a maximum amplitude $\omega_{1S}/2\pi$ = 23.6 kHz and a zero minimum amplitude; a 4 ms delay applied between these two spin-lock pulses. (c) A spin-lock pulse with the amplitude $\omega_{1S}/2\pi$ ramped from 12.5 kHz to 16.7 kHz; (d) MMHH with $\omega_{1I}/2\pi$ = 27.7 kHz and $\omega_{1S}/2\pi$ = 30 kHz. 32 t1 increments were applied for all experiments and the 2D spectra were process using covariance NMR [33].

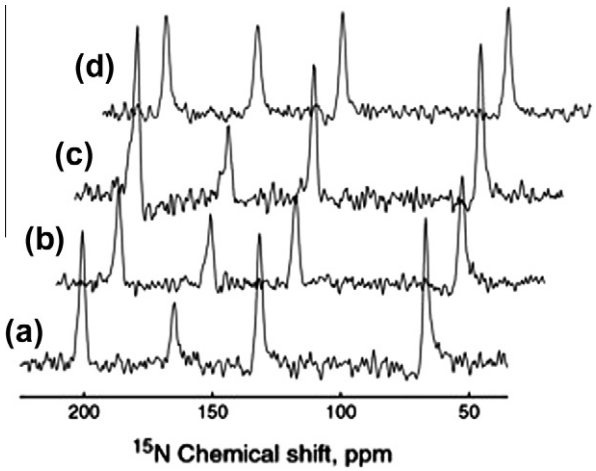

Fig. 4. A comparison of 1D spectral slices extracted from 2D spectra given in Fig. 3. (a–d) Horizontal 1D ^{15}N chemical shift slices taken at 200.9 ppm from the 2D spectra given in Figs. 2a–d; the leftmost peak is the diagonal peak while other peaks are cross peaks.

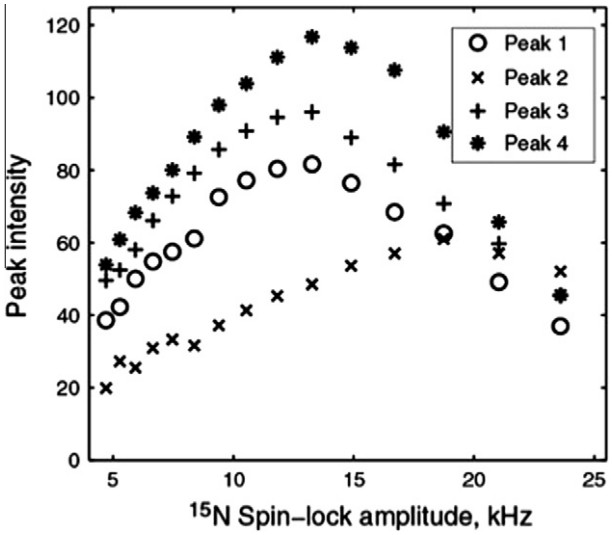

Fig. 5. Peak intensities as a function of $\omega_{1S}/2\pi$ for a 6 ms ^{15}N spin-lock pulse. Dipolar order was created by a direct adiabatic demagnetization of protons by applying a 1 ms ramp pulse (40 kHz to zero). The intensities of peaks 1, 3, and 4 reached a maximum at $\omega_{1S}/2\pi$ = 13.3 kHz; peak 2 intensity reached a maximum at $\omega_{1S}/2\pi$ = 18.7 kHz.

2π = 13.3 kHz whereas the peak 2 reaches a maximum at a higher RF field $\omega_{1S}/2\pi$ = 18.7 kHz. From this, we expect that the pulse sequence given in Fig. 1a will have maximum performance near these values of ω_{1S}. At longer mixing times, the maximum will be reached at higher values of ω_{1S} and will result in larger nitrogen polarization. This conclusion is consistent with our measurements (not shown). The ω_{1S} dependence with a maximum for the CRDSD performance in the NAVL single crystal has also been reported [32].

The relaxation time T_{1D} for the dipolar reservoir can be measured by introducing a delay between the ^{15}N demagnetization and remagnetization as shown in Fig. 1b. Fig. 6 shows the decay of the dipolar order in the NAVL single crystal measured by the ^{15}N remagnetizing pulse applied after a variable delay. The average T_{1D} value obtained from this measurement is about 0.25 s. A slightly different result obtained for different peaks could be due to imperfect adiabatic remagnetization in the experiment. The spin–lattice relaxation time T_{1D} sets a limiting time scale for the mechanism of mixing. In some samples, T_{1D} can be much shorter than T_1.

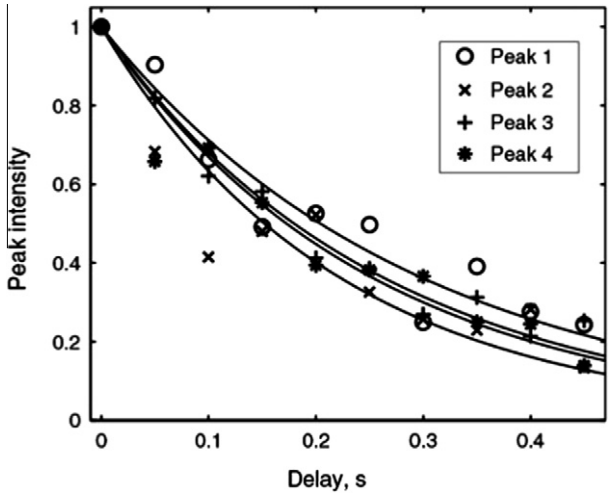

Fig. 6. The decay of the dipolar order in ^{15}N labeled NAVL single crystal, measured by introducing a delay between ^{15}N demagnetization and remagnetizing pulses (Fig. 1b); T_{1D} values, obtained from fitting the peak intensities by exponential decays are 0.29, 0.22, 0.26, and 0.25 s for peaks 1–4, respectively. The peak intensity at time zero was normalized to 1 for all four peaks.

The experimental results (Figs. 3b and 4b) obtained for the pulse sequence given in Fig. 1b is a direct proof that an efficient mixing can occur via an intermediate dipolar-ordered state. A 4 ms RF-free delay was used between the demagnetizing and remagnetizing pulses (in Fig. 1b). The dipolar order is the only type of order that can survive during such a long RF-free interval in this experiment. The main advantage of this pulse sequence is that it is very robust and does not require an optimization of the experimental parameters.

As shown in Figs. 3c and 4c, the performance of the pulse sequence with a ramped spin-lock pulse (depicted in Fig. 1c) is slightly better than the performance of the pulse sequence with a constant-amplitude spin-lock pulse (depicted in Fig. 1a). The ramped pulse also makes it less sensitive to the optimized value of ω_{1S}.

For the MMHH pulse sequence shown in Fig. 1d, the dependence of its performance on the Hartmann–Hahn (HH) mismatch is shown in Fig. 7a. In the experimental result shown in Fig. 7, the RF amplitude applied for ^{15}N was fixed at $\omega_{1S}/2\pi = 30$ kHz. Fig. 7a displays the sum-projected intensities of the four peaks as a function of the amplitude $\omega_{1I}/2\pi$ of the RF field applied on protons. All peak intensities reach a minimum at the exact match $\omega_{1I} = \omega_{1S}$. The efficiency of creating cross-correlation peaks can be seen in Fig. 7b. Again, the intensities of the cross-peaks are the smallest near the match (indicated as ω_3 in Fig. 7b). It is interesting that at $\omega_{1I} = \omega_{1S}$ the intensities are small but not zero, as we would expect from our thermodynamic description. The reason is that, in addition to the ZDZ-mixing, there is also Zeeman–Zeeman–Zeeman (ZZZ) mixing when the ^{15}N polarization is transferred to proton polarization and then back to ^{15}N polarization. This type of mixing has the same mechanism as the Hartmann–Hahn CP. While the ZDZ-mixing increases with HH mismatch, the ZZZ-mixing has a maximum rate near the exact match. One can see in Fig. 7b that the mixing via the dipolar reservoir is more efficient for a static sample. This situation changes under MAS which suppresses the dipolar reservoir and the ZDZ-mixing mechanism leaving the ZZZ-mixing as the dominant mechanism.

3.2. MAS

For a better comparison with the static case, we used a powder sample of NAVL for MAS experiments. A moderate spinning speed of 10 kHz, not compromising the efficiency of ramped-CP, was chosen. Fig. 8a shows a 2D ^{15}N–15N correlation spectrum, recorded with the MMHH pulse sequence depicted in Fig. 7d. The mixing time was only 5 ms. Intensities of both the diagonal and cross-peaks can be improved by using a 90% ramped proton pulse, as it is illustrated in Fig. 8b. The expected mechanism of mixing in this case is the HH-CP. The better performance of the ramped-CP can be explained by inhomogeneities of the two RF fields, created by different coils in the probe. To explore the mixing mechanism in more detail, we compared the dependences on the HH mismatch of a 2 ms CP performance and of the intensities of the diagonal and cross-peaks in the 2D correlation experiment with a 5 ms mixing time. The results are presented in Fig. 9. The CP performance (shown in Fig. 9a) is irregular (due to many factors, including RF field inhomogeneity) but shows distinct maxima at mismatches $|\omega_{1I} - \omega_{1S}| = 0$, 10 kHz. The diagonal peak in Fig. 9b, expectedly, shows maxima in the areas where CP is less efficient. When the CP mechanism is turned off, the nitrogen magnetization is simply locked by the spin-lock pulse. On the contrary, the cross-peaks are high in the regions where the CP efficiency is high (Fig. 9c).

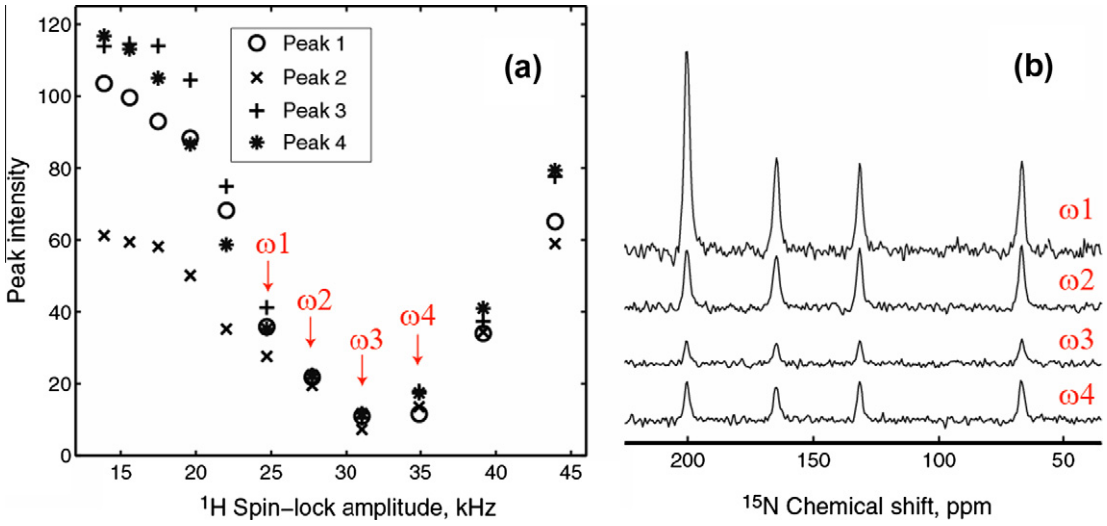

Fig. 7. (a) Integral (projected) intensities of the peaks for 10 ms MMHH as a function of $\omega_{1I}/2\pi$ with $\omega_{1S}/2\pi$ fixed at 30 kHz; (b) horizontal 1D slices taken from the 2D MMHH spectrum (200.9 ppm) that were obtained using $\omega_{1I}/2\pi = 24.7$, 27.7, 31.1, and 34.8 kHz.

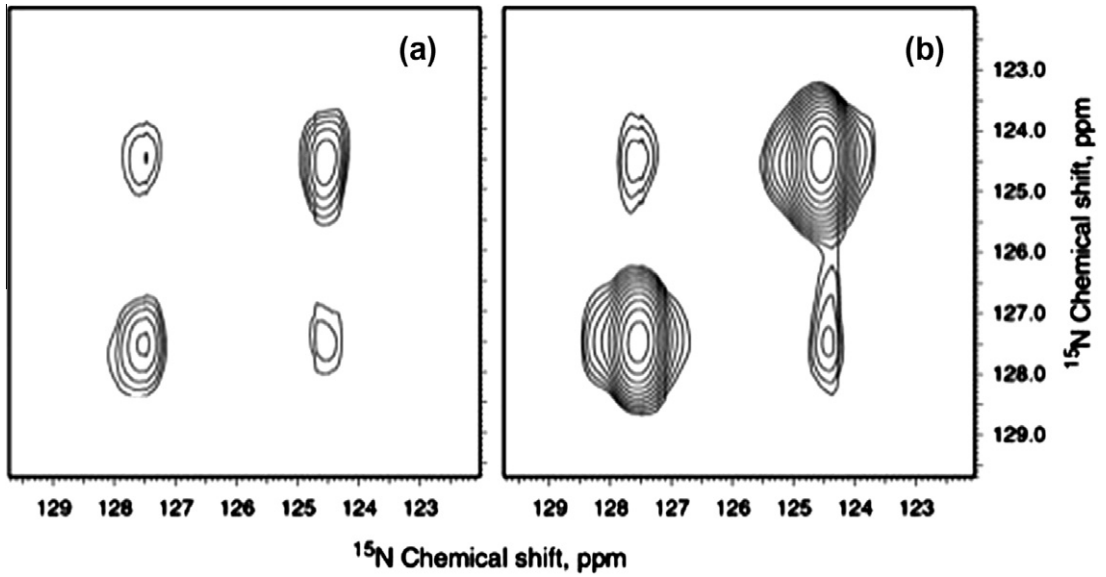

Fig. 8. 2D ^{15}N–^{15}N correlation spectra of NAVL powder under 10 kHz MAS obtained using (a) a pulse sequence shown in Fig. 1d with $\omega_{1I}/2\pi$ = 36 kHz, $\omega_{1S}/2\pi$ = 37 kHz, and (b) the same pulse sequence with a 90% ramp-up proton spin-lock pulse, a maximum of $\omega_{1I}/2\pi$ = 36 kHz, $\omega_{1S}/2\pi$ = 37 kHz. A mixing time of 5 ms was applied for both pulse sequences.

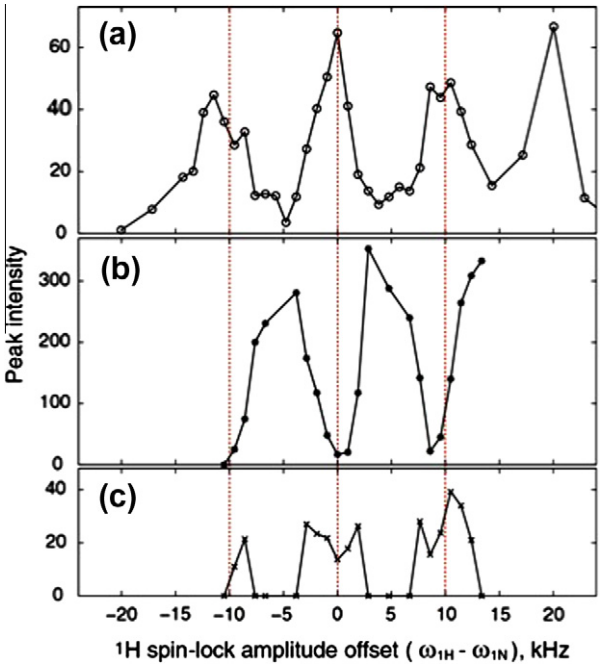

Fig. 9. (a) The ^{15}N CPMAS signal intensity with respect to the proton spin-lock amplitude, while the ^{15}N spin-lock pulse amplitude was fixed at 37 kHz. A 2 ms CP time was used. The diagonal peak intensity (b) and the cross peak intensity (c) of the 2D correlation spectra (at 127.19 ppm) obtained using the PAR pulse sequence with a 5 ms mixing time, 37 kHz ^{15}N spin-lock, and varying the proton spin-lock amplitude. 10 kHz MAS and 55 kHz TPPM decoupling were used in all experiments.

Arbitrary vertical scales was chosen in Fig. 9, but the scales in Fig. 9b and c show the relative intensities of the diagonal and cross-peak.

Even though the explanation of the mixing mechanism by the HH-CP alone is roughly consistent with the experimental observations, Fig. 9 reveals some interesting details. As an example, the CP dependence in Fig. 9a has a very sharp maximum at the exact HH match $\omega_{1I} - \omega_{1S} = 0$. At the same time, the intensity of the cross-peak has a local minimum at the exact match. Cross-peaks are higher at few kilohertz offsets. This may be an indirect indication that the mixing via a reservoir of pseudo-dipolar couplings [26] also contributes to the process. If this is the case, an explanation of the local minimum in Fig. 9c can be similar to the one for the local minimum in Fig. 7b.

4. Conclusions

Our study demonstrated that for static samples, fast and efficient mixing to create cross-correlation of weakly coupled ^{15}N or ^{13}C spins can be achieved by converting the Zeeman order of these spins into a common dipolar reservoir (with heat capacity mostly contributed by protons) and then back to the Zeeman order of ^{15}N or ^{13}C spins. We have shown that there is a common mechanism of mixing for various CRDSD sequences and that the mechanism can be explained in terms of spin thermodynamics. Since the efficiency of building cross-peaks decreases at dilution, as it is predicted by Eq. (4), the CRDSD techniques described in this study are mostly suited for uniformly labeled systems. While the cross-correlation growth curves important for distance estimations and cannot be derived from equilibrium thermodynamics, a concept of spatially inhomogeneous spin temperature and its time-evolution may be a useful tool for semi-quantitative description; simulation of the spin diffusion process could provide insights into the pulse sequences reported in this study [34]. Our results show that the direct Hartman–Hahn cross-polarization remains the main mixing mechanism under MAS as the dipolar bath disappears. There is also a possibility that, under fast-MAS, mixing can be facilitated by a thermal contact with the reservoir of pseudo-dipolar couplings. Scalar couplings, which are relatively weak in static solids, can also provide useful mixing mechanisms under fast MAS.

Acknowledgments

A.K.K. was a visiting Professor at the University of Michigan during his sabbatical leave. We thank Rui Huang for help with some of the experimental measurements. This study was supported by research funds from NIH (GM084018 and GM095640 to A.R.).

References

[1] R. Tycko, G. Dabbagh, Double-quantum filtering in magic angle spinning NMR spectroscopy: an approach to spectra simplification and molecular structure determination, J. Am. Chem. Soc. 113 (1991) 9444–9448.

[2] A.E. Bennett, J.H. Ok, R.G. Griffin, S. Vega, Chemical shift correlation spectroscopy in rotating solids: radio frequency driven dipolar recoupling and longitudinal exchange, J. Chem. Phys. 96 (1992) 8624–8627.

[3] T. Fujiwara, A. Ramamoorthy, K. Nagayama, K. Hioka, T. Fujito, Dipolar HOHAHA under MAS conditions for solid-state NMR, Chem. Phys. Lett. 212 (1993) 81–84.

[4] I. Scholz, M. Huber, T. Manolikas, B.H. Meier, M. Ernst, MIRROR recoupling and its application to spin diffusion under fast magic-angle spinning, Chem. Phys. Lett. 460 (2008) 278–283.

[5] I. Scholz, B.H. Meier, M. Ernst, NMR polarization transfer by second-order resonant recoupling: RESORT, Chem. Phys. Lett. 485 (2010) 335–342.

[6] M. Weingarth, D. Demco, G. Bodenhausen, P. Tekely, Improved magnetization transfer in solid-state NMR with fast magic angle spinning, Chem. Phys. Lett. 469 (2009) 342–348.

[7] N.M. Szeverenyi, M.J. Sullivan, G.E. Maciel, Observation of spin exchange by two-dimensional Fourier transform ^{13}C cross polarization-magic-angle spinning, J. Magn. Reson. 47 (1982) 457–462.

[8] K. Takegoshi, S. Nakamura, T. Terao, C-13–H-1 dipolar-assisted rotational resonance in magic-angle spinning NMR, Chem. Phys. Lett. 344 (2001) 631–637.

[9] T.I. Igumenova, A.E. McDermott, K.W. Zilm, R.W. Martin, E.K. Paulson, A.J. Wand, Assignments of carbon NMR resonances for microcrystalline ubiquitin, J. Am. Chem. Soc. 126 (2004) 6720–6727.

[10] N. Giraud, M. Blackledge, A. Bockmann, L. Emsley, The influence of nitrogen-15 proton-driven spin diffusion on the measurement of nitrogen-15 longitudinal relaxation times, J. Magn. Reson. 184 (2007) 51–61.

[11] A. Ramamoorthy, L.M. Gierasch, S.J. Opella, Four-dimensional solid-state NMR experiment that correlates the chemical-shift and dipolar-coupling frequencies of two heteronuclei with the exchange of dilute-spin magnetization, J. Magn. Reson. B 112 (1995) 6.

[12] A. Ramamoorthy, L.M. Gierasch, S.J. Opella, Three-dimensional solid-state NMR correlation experiment with ^{1}H homonuclear spin exchange, J. Magn. Reson. B 111 (1996) 81.

[13] M. Wilhelm, H. Feng, U. Tracht, H.W. Spiess, 2D CP/MAS ^{13}C isotropic chemical shift correlation established by ^{1}H spin diffusion, J. Magn. Reson. 134 (1998) 255–260.

[14] F.M. Mulder, W. Heinen, M. van Duin, J. Lugtenburg, H.J.M. de Groot, Spin diffusion with ^{13}C selection and detection for the characterization of morphology in labeled polymer blends with MAS NMR, J. Am. Chem. Soc. 120 (1998) 12891–12894.

[15] Y.F. Wei, A. Ramamoorthy, 2D^{15}N–^{15}N isotropic chemical shift correlation established by^{1}H–^{1}H dipolar coherence transfer in biological solids, Chem. Phys. Lett. 342 (2001) 312–316.

[16] A. Lange, S. Luca, M. Baldus, Structural constraints from proton-mediated rare spin correlation spectroscopy in rotating solids, J. Am. Chem. Soc. 124 (2002) 9704–9705.

[17] J. Xu, J. Struppe, A. Ramamoorthy, Two-dimensional homonuclear chemical shift correlation established by the cross-relaxation driven spin diffusion in solids, J. Chem. Phys. 128 (2008) 052308.

[18] A.A. Nevzorov, Mismatched Hartmann–Hahn cause proton-mediated internuclear magnetization transfer between dilute low-spin nuclei in NMR of static solids, J. Am. Chem. Soc. 130 (2008) 11282–11283.

[19] A.A. Nevzorov, High-resolution local field spectroscopy with internuclear correlations, J. Magn. Reson. 201 (2009) 111–114.

[20] J.R. Lewandowski, G. De Paepe, M.T. Eddy, R.G. Griffin, ^{15}N–^{15}N proton assisted recoupling in magic angle spinning NMR, J. Am. Chem. Soc. 131 (2009) 5769–5776.

[21] J.R. Lewandowski, G. De Paepe, M.T. Eddy, J. Struppe, W. Maas, R.G. Griffin, Proton assisted recoupling at high spinning frequencies, J. Phys. Chem. B 113 (2009) 9062–9069.

[22] M. Goldman, Spin Temperature and Nuclear Magnetic Resonance in Solids, Clarendon, Oxford, 1970.

[23] A. Abragam, M. Goldman, Nuclear Magnetism: Order and Disorder, Clarendon, Oxford, 1982.

[24] J.S. Lee, A.K. Khitrin, Thermodynamics of Adiabatic Cross-Polarization, 2008; J. Chem. Phys. 128 (2008) 114504.

[25] G. De Paepe, J. Lewandowski, A. Locquet, A. Bockmann, R.G. Griffin, Proton assisted recoupling and protein structure determination, J. Chem. Phys. 129 (2008) 245101.

[26] T. Charpentier, F.S. Dzheparov, J.-F. Jacquinot, J. Virlet, Dipolar order under fast magic-angle spinning, Chem. Phys. Lett. 352 (2002) 447–453.

[27] J. Jeener, P. Broekaert, Phys. Rev. 157 (1967) 232.

[28] T. Charpentier, J.F. Jacquinot, J. Virlet, F. Dzheparov, Cross polarization under fast magic-angle spinning via dipolar order, in: 43rd Rocky Mountain Conference, Denver CO, 1 August 2001.

[29] R. Ohashi, K. Takegoshi, T. Terao, Cross polarization via the non-Zeeman spin reservoirs under MAS, Solid State Nucl. Magn. Reson. 31 (2007) 115–118.

[30] J.-S. Lee, A.K. Khitrin, Adiabatic cross-polarization via intermediate dipolar-ordered state, J. Magn. Reson. 177 (2005) 152–154.

[31] B.M. Fung, A.K. Khitrin, K. Ermolaev, An improved broadband decoupling sequence for liquid crystals and solids, J. Magn. Reson. 142 (2002) 97–101.

[32] N.J. Traaseth, T. Gopinath, G. Veglia, On the performance of spin diffusion NMR techniques in oriented solids: prospects for resonance assignments and distance measurements from separated local field experiments, J. Phys. Chem. B 114 (2010) 13872–13880.

[33] R. Brüschweiler, F. Zhang, Covariance nuclear magnetic resonance spectroscopy, J. Chem. Phys. 120 (2004) 5253–5260.

[34] J.-N. Dumez, M.C. Butler, E. Salager, B.E. Herrmann, L. Emsley, *Ab initio* simulation of proton spin diffusion, Phys. Chem. Chem. Phys. 12 (2010) 9172–9175.